A dual role of FGF10 in proliferation and coordinated migration of epithelial leading edge cells during mouse eyelid development

Hirotaka Tao[1,*], Miyuki Shimizu[1], Ryo Kusumoto[1], Katsuhiko Ono[2], Sumihare Noji[1] and Hideyo Ohuchi[1,†]

[1]Department of Biological Science and Technology, Faculty of Engineering, University of Tokushima, 2-1 Minami-Jyosanjima, Tokushima 770-8506, Japan
[2]Division of Neurobiology and Bioinformatics, National Institute for Physiological Sciences, Okazaki 444-8787, Japan
*Present address: Department of Developmental Biology, National Institute for Basic Biology, Okazaki 444-8585, Japan
†Author for correspondence (e-mail: hohuchi@bio.tokushima-u.ac.jp)

Accepted 9 May 2005

Development 132, 3217-3230
Published by The Company of Biologists 2005
doi:10.1242/dev.01892

Summary

The development of the eyelid requires coordinated cellular processes of proliferation, cell shape changes, migration and cell death. Mutant mice deficient in the fibroblast growth factor 10 (*Fgf10*) gene exhibit open-eyelids at birth. To elucidate the roles of FGF10 during eyelid formation, we examined the expression pattern of *Fgf10* during eyelid formation and the phenotype of *Fgf10*-null eyelids in detail. *Fgf10* is expressed by mesenchymal cells just beneath the protruding epidermal cells of the nascent eyelid. However, *Fgf10*-null epithelial cells running though the eyelid groove do not exhibit typical cuboid shape or sufficient proliferation. Furthermore, peridermal clumps are not maintained on the eyelid leading edge, and epithelial extension does not occur. At the cellular level, the accumulation of actin fibers is not observed in the mutant epithelial leading edge. The expression of activin/inhibin βB (*ActβB/Inhbb*) and transforming growth factor α (*Tgfa*), previously reported to be crucial for eyelid development, is down-regulated in the mutant leading edge, while the onset of sonic hedgehog (*Shh*) expression is delayed on the mutant eyelid margin. Explant cultures of mouse eyelid primordia shows that the open-eyelid phenotype of the mutant is reduced by exogenous FGF10 protein, and that the expression of *ActβB* and *Tgfa* is ectopically induced in the thickened eyelid epithelium by the FGF10 protein. These results indicate a dual role of FGF10 in mouse eyelid development, for both proliferation and coordinated migration of eyelid epithelial cells by reorganization of the cytoskeleton, through the regulation of activin, TGFα and SHH signaling.

Key words: *Fgf10*, *Shh,* activin βB, *Tgfa,* periderm, mesenchyme, epidermis, mouse, eyelid development, leading edge, cell migration

Introduction

During normal development in mammals, the eyelids grow across the eye, fuse and subsequently reopen. In mice, eyelid formation begins on day 11.5 of gestation (E11.5), and from E14 to 16 the eyelids grow, flatten across the eye, progressively meet beginning at the inner and outer canthi and fuse tightly with each other (Harris and McLeod, 1982; Li et al., 2001). The eyelashes and the glands lying along the margins of the lids start to differentiate from this common epithelial lamina before the lids reopen at 14 days after birth (Findlater et al., 1993).

The developing eyelids are composed of loose mesenchyme covered by an epithelial sheet, the epidermis (outer surface) and conjunctiva (inner surface) and the periderm, which covers the epidermis (Weiss and Zelickson, 1975). Only the peridermal and epidermal layers are involved in eyelid fusion; the mesenchymal layers of the upper and lower eyelids remain separate (Pei and Rhodin, 1970). A profusion of rounded periderm cells appears, and they pile up at the leading edges of the advancing eyelids during eyelid growth (Harris and McLeod, 1982; Harris and Juriloff, 1986; Juriloff and Harris, 1989). Once contact is made between the apposed eyelids, these cells flatten and form a strip along the fusion line, until they slough off with the rest of the periderm on day 17 of gestation (Harris and Juriloff, 1986; Juriloff and Harris, 1989; Findlater et al., 1993).

Failure of the eyelids to grow across the eye and fuse during the fetal stage in mice leads to a birth defect of open-eyelids at birth. Mutations at several distinct loci have been found to cause such open-eyelids, often as part of a syndrome with other defects. For example, open-eyelids results from spontaneous or gene-knockout mutation at the loci of transforming growth factor α (*Tgfa*), its receptor epidermal growth factor receptor (*Egfr*), activin/inhibin βB (*Inhbb* – Mouse Genome Informatics) fibroblast growth factor receptor type 2b (*Fgfr2b*), *Jun*, *MEK kinase 1* and some forkhead genes (Luetteke et al., 1993; Mann et al., 1993; Miettinen et al., 1999; Thereadgill et al., 1995; Vassalli et al., 1994; Celli et al., 1998; De Moerlooze et al., 2000; Li et al., 2001; Li et al., 2003; Zenz et al., 2003; Zhang et al., 2003; Kume et al., 1998; Uda et al., 2004). However, the molecular and cellular events occurring during eyelid development and the interactions among the signaling molecules have not been fully elucidated. We previously reported briefly that *Fgf10*-null mice exhibit open-eyelids at

birth with multi-organ developmental defects (Sekine et al., 1999; Ohuchi et al., 2000). Here, we report the expression pattern of *Fgf10* during eyelid formation and the phenotype of *Fgf10*-null eyelids in detail. We found that FGF10 is dually required for proliferation and coordinated migration of epithelial cells during mouse eyelid development by reorganization of the cytoskeleton, through the regulation of activin, TGFα and SHH signaling.

Materials and methods

Mice

Fgf10-knockout mice were generated on a C57BL/6 × CBA background and genotyped as previously described (Sekine et al., 1999). In the *Fgf10*-null mice, the phenotype of open-eyelids at birth is seen in homozygotes, while the eyelids of heterozygotes appear normal at birth, as reported previously (Sekine et al., 1999). So far, all examined homozygous mice have exhibited open-eyelids at birth. Noon of the day when the vaginal plug was detected was considered embryonic day 0.5 (E0.5) of development for embryos of the overnight mating. For analysis of eyelid morphogenesis, the heads of $Fgf10^{-/-}$, $Fgf10^{+/-}$ and wild-type mice were collected at the desired stages (n=3~5 for each genotype and stage). For analysis of the normal expression patterns of *Fgf10* and other genes, the heads of *Slc:ddy* mice (no pigment in the eye) (Japan SLC, Inc.) were used at the desired stages (n=3 for each stage).

Histology and electron microscopy

For histological analysis, Hematoxylin and Eosin (HE) staining was performed according to the standard procedure.

The $Fgf10^{+/+}$, $Fgf10^{+/-}$ and $Fgf10^{-/-}$ embryos at around E15 and E16 (n=3~6 for each genotype and stage) were fixed in 4% paraformaldehyde (PFA)/5% glutaraldehyde/PBS (10 mM phosphate-buffered saline) overnight and processed for scanning or transmission electron microscopy observation according to standard procedures.

In situ hybridization

Normal and $Fgf10^{-/-}$ mutant embryos at the desired stages were fixed in 4% PFA in PBS overnight and used for in situ hybridization. Digoxigenin-labeled riboprobes for mouse *Fgf10*, *Shh* (Sekine et al., 1999), Patched (*Ptch1*), *Ptch2* (Motoyama et al., 1998) and activin βB (provided by Dr Tsuchida, University of Tokushima, Japan) were prepared as described. The mouse *Tgfa* cDNA (*Tgfa*; 2578 bp) was isolated by RT-PCR using E18.5 mouse whisker mRNA. The PCR primers were as follows: the sense primer was 5′-tgtgtctgccac-tctgggtacgtg-3′ and the antisense primer was 5′-aacgcagcagggctgtca-tacgtc-3′. Sense probes were used as a control and produced virtually no signals. Whole-mount in situ hybridization was performed as previously described (Tao et al., 2002). Section in situ hybridization was performed on 18-μm thick frozen sections according to standard procedures, or by using a tyramide signal amplification method on 7-μm thick paraffin sections (Yang et al., 1999). The gene expression patterns were compared between littermates, and the in situ hybridization experiment was repeated at least three times for each gene.

RT-PCR

Total RNA was isolated from the back skin (of normal E18.5 mice), wild-type and *Fgf10*-null keratinocytes (at E18.5) and eyelid mesenchyme [of normal mice at E15, treated with Dispase II (Roche) to remove epithelial tissues] by using an RNAqueous Kit (Ambion). To prevent contamination of the genomic DNA, the samples were treated with RNase-free DNase (Promega). The DNase was subsequently inactivated at 70°C for 5 minutes, and the samples were subjected to chloroform/phenol extraction and ethanol precipitation. Reverse transcription (RT) was carried out using 1 μg of total RNA, Superscript II reverse transcriptase (Invitrogen), and gene-specific primers as follows: MA-5′ primer (ATGACCCAGATCATGTTTG-AGACC) and MA-3′ primer (AGGAGGAGCAATGATCTTGAT-CTT) for β-actin (645 bp); *Fgf10*-Se primer (AAGCTCTTGGT-CAGGACATGG) and *Fgf10*-An primer (ATGGGGAGGAAGTGA-GCAGA) for *Fgf10* (506 bp); and *Fgfr2b*-Se primer (ACA-CCGAGAAGATGGAGAAG) and *Fgfr2b*-An primer (GTTTG-GGCAGGACAGTGAG) for *Fgfr2b* (609 bp). PCR was performed using Ex Taq polymerase HS (Takara Bio, Japan) and 1/10 of the volume of the cDNA reaction mix. In total, 35 cycles were performed at annealing temperatures of 60°C for *Fgf10* and 65°C for *Fgfr2b*. The analysis was repeated twice with samples from two different fetuses for each genotype, and all gave the same results.

BrdU incorporation, quantitative histomorphometry and TUNEL assay

To analyze BrdU uptake in embryos, pregnant mice were injected intraperitoneally with BrdU (Roche) at a dose of 100 μg/g body weight and were sacrificed 1 hour later. Immunohistochemical staining for BrdU was performed using a monoclonal antibody (G3G4, 1:100) from Developmental Studies Hybridoma Bank, a M.O.M. kit (Vector) and a NovaRed substrate (Vector) according to the manufacturers' instructions. At E11.5, the BrdU-positive cells were counted in the epithelium (along the line shown in Fig. 4A,B, approximately 200 μm long in each eyelid) and in three serial sections (21 μm) for each embryo (wild type, n=5; $Fgf10^{-/-}$, n=4). Since the total number of cells was not found to differ between genotypes, the number of BrdU-positive cells did not reflect varying cell density. The epithelial areas counted for BrdU-positive cells at E13.5 are indicated in Fig. 4D,E. The percentage of BrdU-positive cells was calculated (wild type, n=3; $Fgf10^{-/-}$, n=3). The epithelial areas counted for BrdU-positive cells at E15 are indicated in Fig. 4I,J. The percentage of BrdU-positive cells was again calculated (wild type, n=4; $Fgf10^{-/-}$, n=3). The means and standard errors of the means (s.e.m.) were calculated from the pooled data. Differences were judged significant if P<0.05 (as shown by the asterisks in Fig. 4), as determined by Student's t-test.

A TUNEL assay of apoptotic cells on tissue sections was carried out as recommended by the manufacturer (ApopTag, Intergen). The sections were pretreated with 0.5% Triton X-100, and diaminobenzidine was used as a substrate for horseradish peroxidase.

Immunofluorescence

Immunostaining for γ-tubulin was performed essentially according to the procedure of Thompson et al. (Thompson et al., 2004). Briefly, heads from wild-type and *Fgf10*-deficient embryos at around E15 were cut at the midline and fixed overnight in 3% formaldehyde in PBS after Triton X-100/PEG treatment (Libusova et al., 2004). Cryosections with a thickness of 18 μm were prepared and processed for immunofluorescence. The anti-γ-tubulin (Clone GTU-88; Sigma, diluted at 1:1000) and anti-vimentin (Clone Vim3B4; Dako, diluted at 1:200) monoclonal antibodies were visualized by using Cy3-conjugated goat anti-mouse IgG (Jackson, diluted at 1:1000). To illuminate the cell boundaries, Bodipy-ceramide (FLC5; Molecular Probes) was used, according to Lele et al. (Lele et al., 2002), at a concentration of 10 μM. The number of γ-tubulin-expressing cells in the basal epidermis of the eyelid tip (approximately 17 cells along the broken line shown in Fig. 7J,K) was calculated.

Staining for F-actin of flat mounts and frozen sections (18 μm) was carried out using eye samples from E15 embryos fixed in 4% paraformaldehyde. The tissues were incubated with Rhodamine-phalloidin (Molecular Probes) and observed with a fluorescence stereomicroscope (Leica) or by laser scanning confocal microscopy (BioRad) according to standard procedures.

Isolation and culturing of primary keratinocytes and in vitro scratch assay

Isolation and culturing of primary keratinocytes were performed basically according to Li et al. (Li et al., 2003) with minor modifications. Briefly, E18 embryos were collected, and their skin removed, washed and incubated in Dispase medium [defined keratinocyte-serum free medium (DK-SFM; Invitrogen), 5 U/ml Dispase II, 100 μg/ml streptomycin, 0.25 μg/ml fungizone, 50 μg/ml gentamicin] at 4°C for 18 hours. The dermis was separated from the epidermis, and the epidermis was minced and digested in 0.05% trypsin-EDTA for 10 minutes. A mouse keratinocyte culture medium containing DK-SFM, 10 ng/ml EGF (Sigma) and 10 ng/ml choleratoxin (Wako, Japan) was used. In the case of the E18 embryonic keratinocytes, we did not observe a distinct difference in motility with or without EGF.

To determine the cell motility, wild-type and mutant keratinocytes were seeded onto 6-well culture dishes or chamber slides (Nalge Nunc), grown to confluence and transferred to a growth factor-free medium plus mitomycin C (Sigma) for 2 days. The confluent monolayers were wounded using a disposable Pasteur pipette tip (Iwaki, Japan) and EGF was added again. For immunostaining, the cells were washed twice with PBS and fixed in 3.7% formaldehyde solution in PBS for 10 minutes at room temperature.

Explant cultures of mouse eyelid primordia

Eyelids (with the anterior segment of the eye) at E15 were cultured at the air-fluid interface by placing them on 0.4-μm Milli Cell-CM (PICM 03050, Millipore, Bedford, MA, USA) in 6-well plates containing DK-SFM. The organ cultures were maintained at 37°C under 100% humidity and 95% air-5% carbon dioxide for 1 day. Heparin-coated acrylic beads (H5263, Sigma), 250-300 μm in diameter, were incubated in 0.5 mg/ml recombinant human FGF10 (Peprotech) at 37°C or 40 minutes and then stored at 4°C before being placed on the explant. For control experiments, beads were soaked in PBS according the same protocol. An FGF10-soaked bead or PBS-bead was inserted into the eyelid mesenchyme. The distance between the eyelid margin and the bead was estimated, from microscope observation, to be approximately 300 μm.

The eyelid closure percentage was calculated by measuring the area of the epithelium covering the cornea (Fig. 9M) at the beginning of the culture and after 8 hours, using the NIH Image program (http://rsb.info.nih.gov/nih-image/). The means and s.e.m. values were calculated from the pooled data (FGF10-bead, n=3; PBS-bead, n=2).

Results

Fgf10 is expressed in the mesenchyme underlying the nascent eyelid epithelium

The processes of mouse embryonic eyelid development are shown in Fig. 1. They include the following: initiation (ectoderm morphogenesis and groove formation; E11.5), eyelid mesenchymal protrusion (E13.5), protruding epithelial ridge formation at the tip of the eyelid margin (E15) and subsequent extension of the upper and lower eyelid epithelium first (E15~16) and mesenchymal cells later (E16.5~17.5) (Li et al., 2001; Stepp, 1999). The upper and lower eyelid fusion occurs in the epithelium, and the mesenchymal cells are not fused for subsequent reopening. The once-fused eyelid normally re-opens at 2 weeks after birth. As *Fgf10*-null mice die at birth because of the absence of lung formation (Sekine et al., 1999), we speculated that FGF10 might be required for certain developmental steps that lead to eyelid closure.

To specify the role of FGF10 in eyelid development, we sought to determine its expression pattern in mouse eyelid

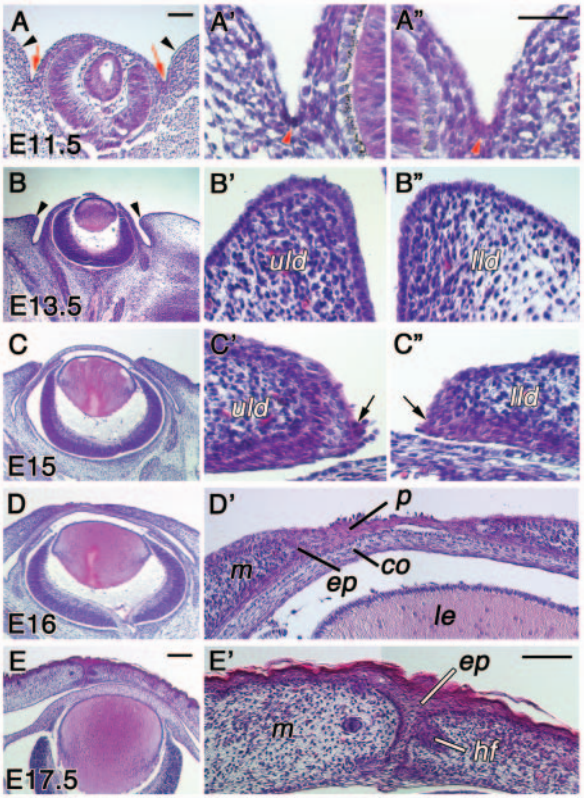

Fig. 1. Eyelid development of the mouse at embryonic day 11.5 (E11.5) (A-A″), E13.5 (B-B″), E15 (C-C″), E16 (D,D′), and E17.5 (E,E′). The upper and lower eyelids are at the left and right, respectively. (A′-E′,A″-C″) Higher magnifications of the eyelid primordia shown in A-E, respectively. (A) The ocular surface epithelium forms small grooves (arrows), and eyelid primordia (arrowheads) begin to emerge. (A′,A″) The epithelial cells at the bottom of the groove have become cuboid (arrowheads). (B) The arrowheads indicate eyelid protrusions. (B′,B″) The eyelid epithelium has become two-layered, with the leading edge cells yet to be formed, while the eyelid dermis starts proliferating. (C-C″) The protruding epithelial ridge has formed at the leading edge (arrow in C′ and C″). (D,D′) The suprabasal epithelial cells between the two lids meet and fuse to form an epithelial bridge. (E,E′) After epithelial fusion, the ocular surface epithelia stratify and differentiate, while the upper and lower lid mesenchyme (m) have extended towards the junctional area and faced each other. co, cornea; ep, epidermis; hf, hair follicle; le, lens; lld, lower eyelid; p, periderm; uld, upper eyelid. Scale bars: A and B′-E′, 100 μm; A′,A″, 50 μm; B-E, 200 μm.

primordia. It has been reported that *Fgf10* is expressed in the mesenchyme of developing eyelids at E12.5 (Li et al., 2001). Its expression domain and profile, however, have not been fully described. Therefore, we re-examined the expression pattern of *Fgf10* until eyelid fusion. At E11.5, *Fgf10* was expressed in the mesenchyme underneath the epithelium of the emerging eyelid groove (Fig. 2A,B). By E13.5, *Fgf10* was expressed in the eyelid mesenchyme just beneath the epithelial tip and in the developing corneal stroma (Fig. 2D-F). At E15, it was expressed around the eye (Fig. 2G), in the eyelid mesenchyme (Fig. 2H,I). By contrast, the major receptor for FGF10 during organogenesis, *Fgfr2b*, was expressed in the eyelid epithelium (Fig. 2J-L). RT-PCR analysis using E18.5 keratinocyte RNA verified that *Fgf10* was not expressed in the epithelium but

Fgfr2b was expressed there (Fig. 2M). These expression patterns suggest that *Fgf10* may be involved in eyelid development from a very early stage, and that in the absence of FGF10 primary defects may be found in the eyelid epithelium.

Defects in the *Fgf10*-null eyelid epithelium at the initiation stage of eyelid development

The *Fgf10*-null embryos had no eyelids at birth, but eyelid protrusion was distinctly observed (Fig. 3C,D; see A,B for control). Taken together with the expression pattern of *Fgf10* described above, FGF10 may be required for maintenance of eyelid formation, rather than for induction of eyelid anlagen. Other significant differences at this stage involved the developing corneal layers. In $Fgf10^{-/-}$ eyes, the corneal stroma appeared less organized (Fig. 3Q). The role of FGF10 in corneal development will be described in detail elsewhere.

To determine which processes require FGF10 during eyelid development, we examined the developmental processes of mutant eyelid primordia by comparing them with normal ones. The initiation stages of eyelid development include ectoderm morphogenesis and groove formation. The ectoderm morphogenesis initiates at E11.5 when the flat ectoderm cells above and below the optic vesicle undergo morphogenetic changes to form cube-shaped epithelial cells. The epithelium also starts to form small eyelid grooves above and below the eye, which were obvious at E11.5 in the wild type (Fig. 3E,F). In the mutant embryos, however, the initial morphogenetic change from flat ectoderm cells to cuboid epithelial cells was not observed, as the mutant cells maintained a flat appearance (Fig. 3G,H). As the eyelid grooves deepened by E13.5 in the wild type, mesenchymal cells nearby started proliferating to form primitive eyelids with protruding ridges of epithelium (Fig. 3I-K). However, the mutant eyelid anlagen appeared much smaller, the groove was shallower and the epithelium overlying the eyelid mesenchyme remained flat (*n*=3; Fig. 3L-N).

To investigate the mechanisms underlying defects of eyelid primordia, we assessed the number of proliferating cells using a BrdU incorporation assay. At E11.5, the mutant epithelium showed a dramatic decrease in proliferation, as only 17.1±1.9 cells incorporated BrdU, while 41.2±2.6 wild-type cells were BrdU positive in the lower eyelid (see Materials and methods; *n*=4; Fig. 4A-C). The number of proliferating cells in the upper eyelid epithelium was significantly reduced as well ($P<0.0005$; Fig. 4C). To check whether the reduced protrusion of the *Fgf10*-null eyelid was exacerbated by an increase in apoptosis, we also analyzed sections using an in situ TUNEL assay. No prominent changes in the apoptotic cell numbers were detected in *Fgf10*-null eyelids compared with their wild-type littermates (data not

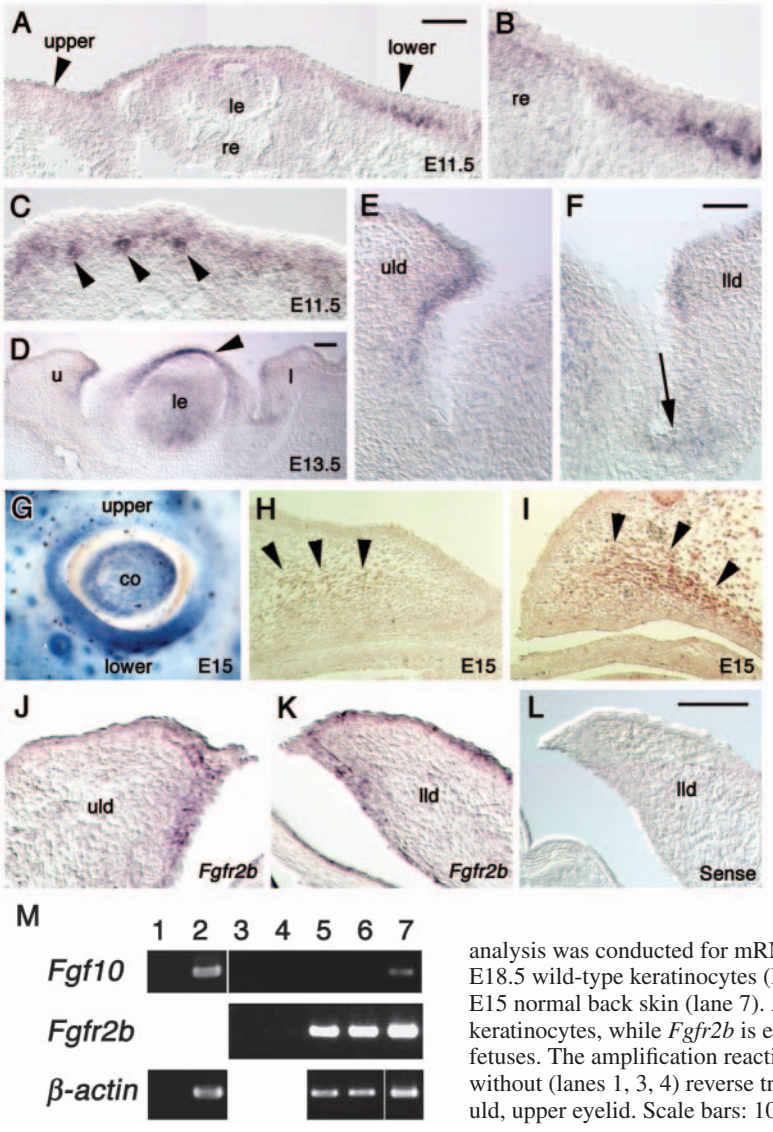

Fig. 2. Expression patterns of *Fgf10* (A-I,M) and *Fgfr2b* (J-L,M) in the developing eyelid. (A) *Fgf10* is expressed in the underlying mesenchyme of the prospective eyelid region (arrowheads). (B) Higher magnification of the lower eyelid region in A. (C) *Fgf10* is expressed in the mesenchyme of the developing whiskers (arrowheads), which is shown as an internal control for in situ hybridization. (D) *Fgf10* is expressed in the mesenchyme underneath the upper (u) and lower (l) eyelid protrusions. The arrowhead indicates *Fgf10* expression in the future corneal stroma. (E,F) Higher magnification of the eyelid protrusion in D. *Fgf10* is expressed in the surrounding mesenchyme at the bottom of the eyelid groove (arrow in F) in addition to the eyelid tip. (G) Whole-mount in situ hybridization of the eye region. *Fgf10* is expressed in the eyelid region and hair follicles. The *Fgf10* expression is more intense in the lower eyelid. The inner canthus (towards the nose) is to the right; the outer canthus (towards the temples) is to the left. (H,I) Section in situ hybridization, showing more intense *Fgf10* expression (arrowheads) in the lower eyelid mesenchyme in (I). (J-L) *Fgfr2b* is expressed in the eyelid epithelium. A sense probe for *Fgfr2b* produces no signals (L). (M) RT-PCR analysis was conducted for mRNA purified from E15 normal eyelid mesenchyme (lanes 1, 2), E18.5 wild-type keratinocytes (lanes 3, 5), E18.5 *Fgf10*-null keratinocytes (lanes 4, 6), and E15 normal back skin (lane 7). *Fgf10* is expressed in the eyelid mesenchyme and not by keratinocytes, while *Fgfr2b* is expressed by keratinocytes from wild-type and *Fgf10*-null fetuses. The amplification reaction was performed after incubation with (lanes 2, 5, 6, 7) or without (lanes 1, 3, 4) reverse transcriptase. co, cornea; le, lens; lld, lower eyelid; re, retina; uld, upper eyelid. Scale bars: 100 μm (A,D); 50 μm (B,C,E,F); 100 μm (H-L).

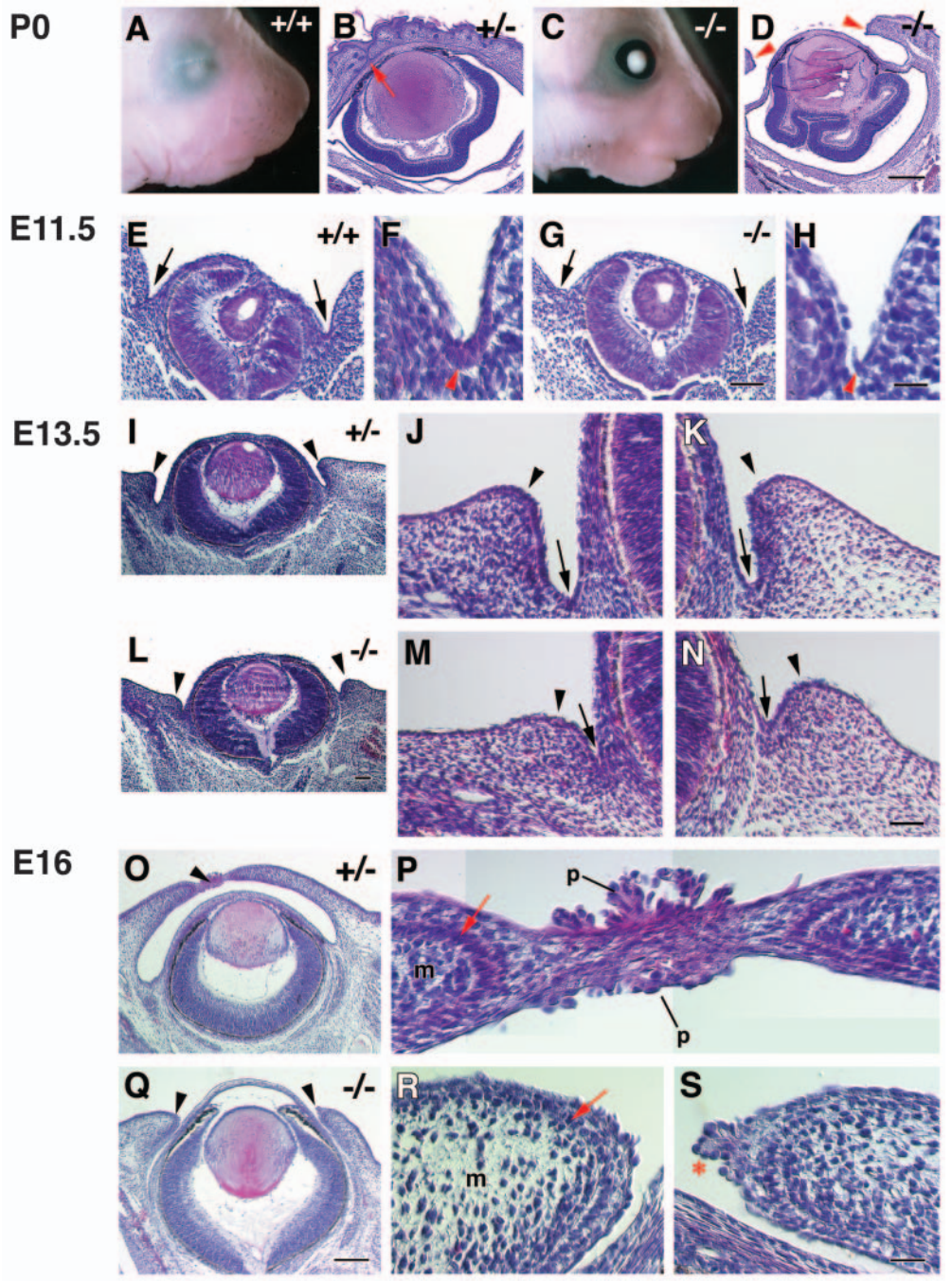

Fig. 3. Eyelid defects in *Fgf10*-null mice. (A,C) Lateral views of the face from wild-type (A) and $Fgf10^{-/-}$ (C) mice at birth. (B,D) Histology of the eyes of $Fgf10^{+/-}$ (B) and $Fgf10^{-/-}$ (D) mice at birth. The upper and lower eyelids are at the left and right, respectively. The $Fgf10^{+/-}$ neonate eyelids are fused (arrow in B), while the *Fgf10*-null eyelids are wide apart (arrowheads in D). The involution of the retina in D is an artifact. (E-S) HE staining of the coronal eye sections from wild-type (E,F), $Fgf10^{+/-}$ (I-K,O,P), and $Fgf10^{-/-}$ (G,H, L-N, and Q-S) embryos at E11.5 (E-H), E13.5 (I-N) and E16 (O-S). (E-H) The arrows in E and G indicate the developing eyelid groove. The epidermal cells at the bottom of the lower groove (arrowhead in F) have become cuboid by this stage in the wild-type mice, while they remain flat in the *Fgf10*-null mice (arrowhead in H). (I-N) The eyelid protrusion (arrowheads) is smaller, and the eyelid groove (arrows) shallower, in the *Fgf10*-null fetuses. (O-S) The arrowheads in O,Q indicate the eyelid leading edge. Eyelid closure is disrupted in *Fgf10*-null fetuses. (P) The junctional region of recently fused eyelids of the $Fgf10^{+/-}$ fetus consists of a loose grouping of cells overlaid by periderm cells (p), which appear to be spilling out onto both the internal and external surfaces. (R,S) The first sign of leading edge cells extending across the corneal surface can be seen in one primitive eyelid (asterisk in S) but not in the other for the *Fgf10*-null fetus. The arrows indicate the basal layer of the eyelid epidermis, which has spindle-shaped nuclei in P and round ones in R. m, mesenchyme. Scale bars: 250 μm (B,D); 100 μm (E and G, F and H, I and L, J,K,M and N,O and Q); 25 μm (P,R and S).

shown). These observations indicate that the loss of *Fgf10* interferes with eyelid formation by E11.5 due to impaired cell proliferation.

Integrity of peridermal clumps is disrupted on the eyelid margin

By E16, the normal eyelids were fused closed (Fig. 3O), whereas the mutant eyelids remained wide apart, above and below the eye, leaving the cornea exposed (Fig. 3Q). Distinct accumulation of periderm cells was seen in the normal eyelid (Fig. 3P). In the mutant eyelid, on the other hand, a protruding ridge was formed at the leading edge of the lower eyelid primordium (Fig. 3S) but did not continue to grow later, and a round malformed eyelid leading edge was often observed in the mutant (Fig. 3R).

Scanning electron microscopy (SEM) observation of E15 normal eyes showed that rounded periderm cells were present in clumps all around the eyelid margin (Fig. 5A; B for $Fgf10^{-/-}$ mutant). In *Fgf10*-null eyelids, however, typical peridermal clumps were merely seen at the inner canthus (Fig. 5D; C for comparison). The periderm cells were rather scattered on the upper and lower eyelid margins of the mutant (Fig. 5F; E for comparison), and they were hardly seen at the outer canthus (Fig. 5H; G for comparison). Transmission electron microscopy further revealed the formation of filopodia in the leading edge periderm cells (Fig. 5I). It is known that filopodia

are pivotal for epithelial fusion: they scan the opposing leading edge, playing an integral role in finally knitting the epithelial hole closed. In the *Fgf10*$^{-/-}$ mutant leading edge, epidermal cells still developed filopodia, although these were distinctly fewer and shorter (Fig. 5J) (n=3). Thus, FGF10 is not required for the formation of filopodia per se during eyelid fusion, but seems necessary for their growth and maturity. At E16, SEM observation verified that the normal eyelids were fused with the epidermis that was streaming towards the point of fusion, where periderm cells accumulated along the junctional region (Fig. 5K). In contrast, wide-open, *Fgf10*-null eyelid rudiments had an epithelial ridge on their margin, whose subsequent growth collapsed (Fig. 5L).

A decrease in proliferating cells of the epithelium was not detected in the *Fgf10*-null epithelium at E15 (Fig. 4I-M), although it was detected at E13.5 (P=0.03) (Fig. 4D-H). The TUNEL assay did not show any differences in the numbers of apoptotic cells between the mutant and normal eyelid territories at either E13.5 or E15 (data not shown). Thus, *Fgf10*-null eyelids fail to maintain peridermal clumps on the lid margin at around E15, which may results from cellular events independent of cell proliferation and apoptosis.

Normal motility in *Fgf10*-null keratinocytes: formation of filopodia and lamellipodia can be observed

It has been reported that cell migration is a crucial process during eyelid epithelial fusion, in which EGF/TGFα and/or

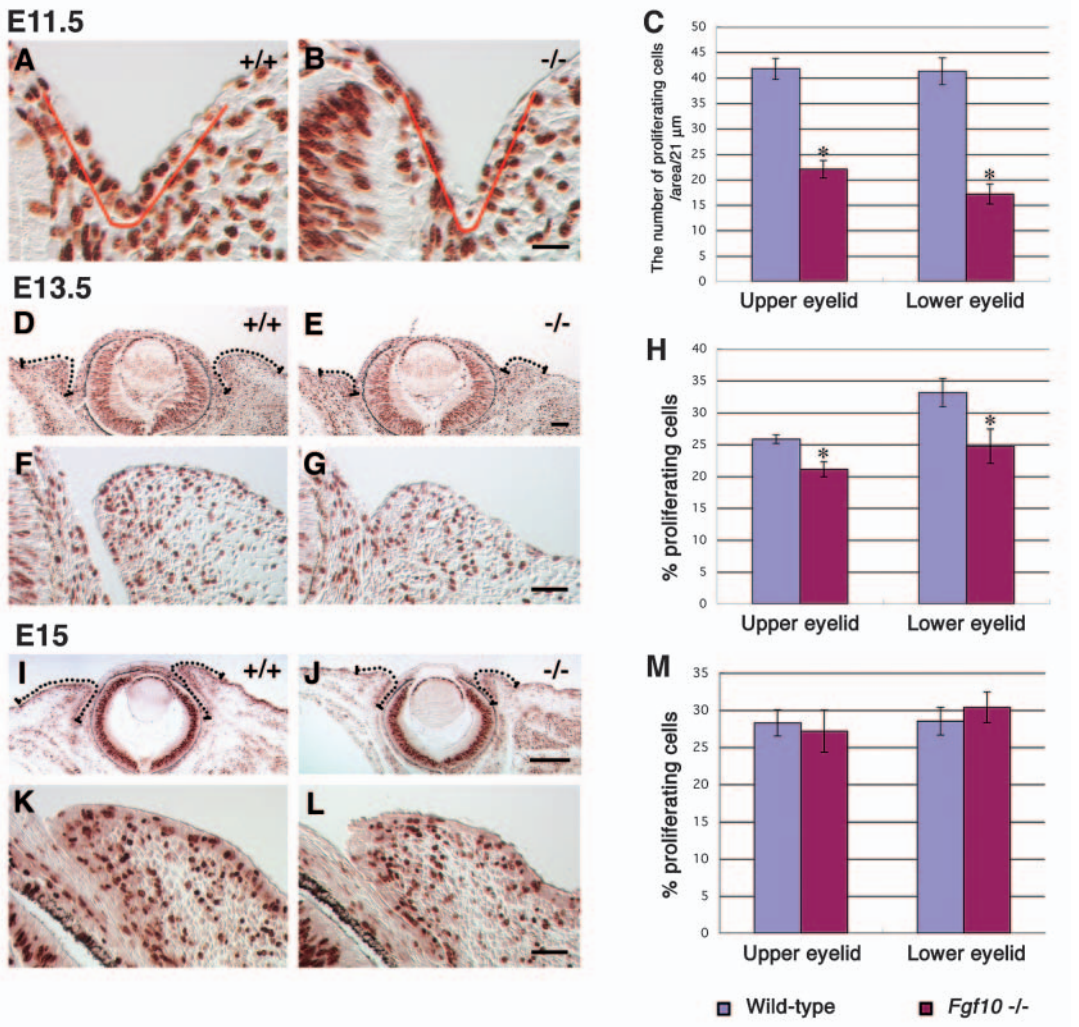

Fig. 4. Cell proliferation in the developing eyelid epithelium in wild-type and *Fgf10*$^{-/-}$ mice. (A-C) BrdU analysis of the E11.5 eyelid. (A,B) Histological sections for BrdU staining. The red line underlies the epithelium where the number of BrdU-positive cells was counted (see Materials and methods for details). (C) The total number of proliferating cells from three sections was processed for quantitative histomorphometry. Compared to wild-type animals, the proliferation in *Fgf10*$^{-/-}$ mutant epithelia was significantly reduced. BrdU incorporation was particularly noticeable in the wild-type eyelid groove, as shown in A. (D-H) BrdU analysis of the E13.5 eyelid. (D-G) Histological sections for BrdU staining. The upper and lower eyelids are at the left and right, respectively. The proliferation rates were significantly reduced in the *Fgf10*$^{-/-}$ mutants. BrdU incorporation was particularly noticeable in the apex region of the wild-type eyelid, as shown in F. (I-M) BrdU analysis of the E15 eyelid. (I-L) Histological sections for BrdU staining. At E15, the *Fgf10*-null upper and lower eyelid epithelia showed no significant decrease in proliferation. In C, H and M the y axes indicate the cell number or mean percentage of BrdU incorporation in each area assayed. The error bars represent the s.e.m.; an asterisk denotes a significant finding (P<0.05), as compared with the wild-type value. In D,E,I,J, the dotted lines indicate the length of epithelium measured. Scale bars: 25 μm (A,B); 100 μm (D,E); 50 μm (F,G); 100 μm (I,J); 50 μm (K,L).

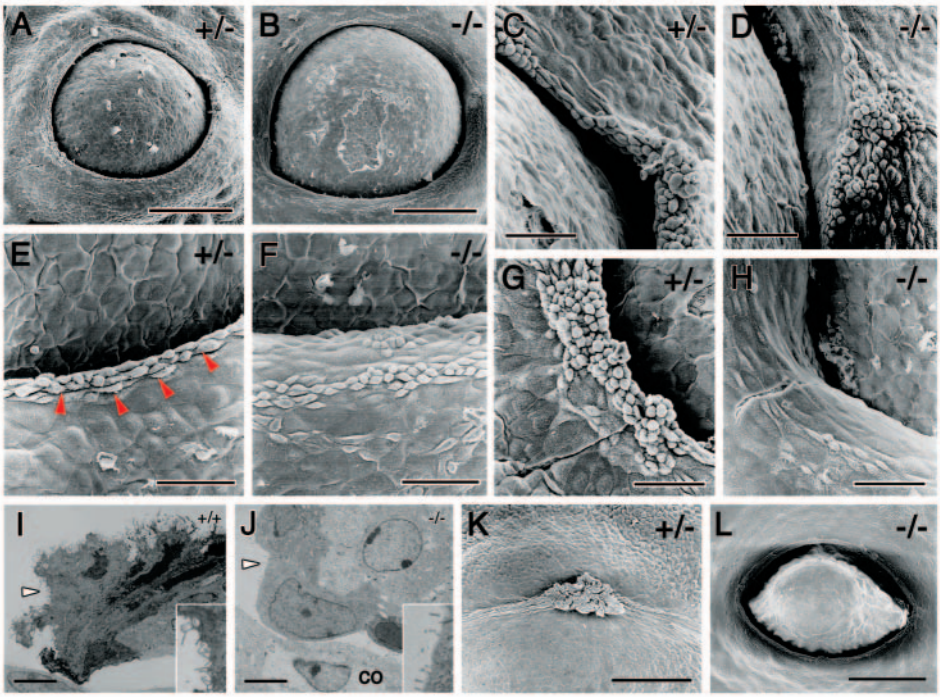

Fig. 5. Scanning electron micrographs of E15 (A-H) and E16 (K, L) eyelids from *Fgf10*$^{+/-}$ (A,C,E,G,K) and *Fgf10*$^{-/-}$ (B,D,F,H,L) fetuses. C,E,G and D,F,H are higher magnifications of A and B, respectively. (C,D) The inner canthus region, (E,F) the lower eyelid margin, and (G,H) the outer canthus region. Clumps of rounded periderm cells are observed in the inner canthus of the *Fgf10*$^{-/-}$ mutant (D), but rarely seen in the outer canthus (H). (E) The arrowheads indicate a regular accumulation of epithelial cells, with the future periderm cells lined up on the eyelid margin of the heterozygote. (F) In the homozygote, rounded periderm cells are scattered away from the eyelid margin. (I,J) Transmission electron micrographs of the eyelid tip epithelium from wild-type (I) and *Fgf10*$^{-/-}$ (J) E15 fetuses. Section near the outer canthus region. Insets show higher magnifications of filopodia of a leading edge cell (indicated by an arrowhead). (I) Numerous filopodia are produced. (J) In the *Fgf10*$^{-/-}$ mutant leading edge, epidermal cells still produce filopodia, although these are distinctly fewer and shorter. co, cornea. (K,L) *Fgf10*$^{+/-}$eyelids are fused, whereas *Fgf10*-null ones are wide open. Scale bars: 380 μm (A,B); 60 μm (C-H); 5 μm (I,J); 300 μm (K); 500 μm (L).

activin-Jun cascades are involved (Li et al., 2003; Zenz et al., 2003; Zhang et al., 2003). Therefore, it is possible that FGF10 controls the epithelial cell migration required for eyelid closure. To assess the role of FGF10 in cell migration during eyelid closure, we isolated primary keratinocytes as major constituents of the eyelid epidermis from wild-type and *Fgf10*-null fetuses, and cultured cells with EGF as the only growth factor supplement. To determine whether FGF10 signaling might be involved in cell migration, we employed an in vitro scratch assay, in which a 'wound' was introduced in cultured monolayers of keratinocytes (Fig. 6A); these cells were cultured in the presence of mitomycin C and were thus mitotically inactive. In the wild-type cultures, the cells responded to the scratch by migrating into the gap and effected closure within 20 hours. The *Fgf10*-null keratinocytes also migrated into the wound in considerable numbers during the same period (Fig. 6A).

We then characterized the migration response to the scratch by observing the cellular levels and distribution of F-actin, which is essential for cell movement. Staining of F-actin with phalloidin (within 5 hours) revealed that in wild-type leading edge cells, the actin distribution was polarized and formed into stress fibers, which accumulated in the anterior lamellipodia oriented toward the wound (Fig. 6B). In *Fgf10*-null cells, the formation of lamellipodia was observed, but their orientation appeared rather irregular; they did not face the gap (Fig. 6C). The formation of filopodia scanning the opposing leading edge was discernible in the mutant as well as the wild type (Fig. 6D,E). The filopodia in the mutant cells, however, appeared thinner than those in the wild-type cells. Thus, *Fgf10*-null

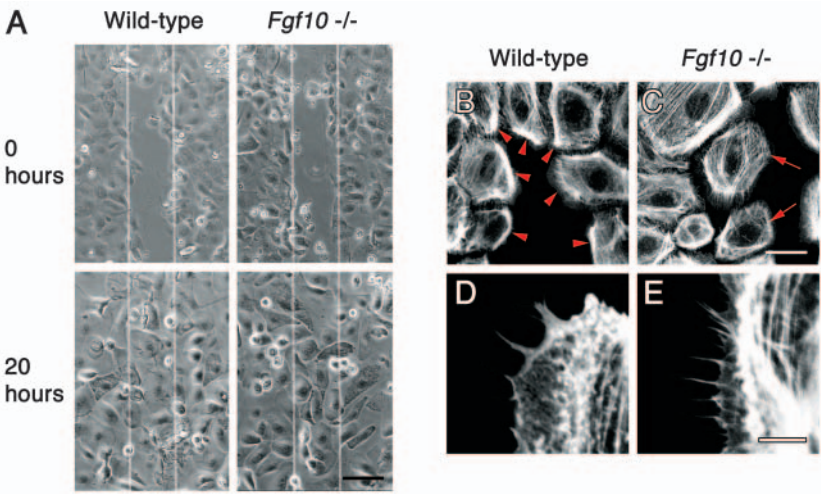

Fig. 6. Cultures and analyses of primary keratinocytes. (A) In vitro scratch assay. Both the wild-type and mutant keratinocytes migrated into the gap within 20 hours. (B-E) Laser scanning microscopic analysis of actin organization in wild-type and mutant keratinocytes at the leading edge of a scratch assay performed as above 5 hours post-scratch. The cells were fixed and stained with phalloidin. Lamellipodia (B,C) and filopodia (D,E) are observed in both the wild-type and mutant keratinocytes, although in the mutant the lamellipodia are often not oriented toward the gap (arrows in C; arrowheads in B for comparison) and the filopodia appear thinner. Scale bars: 100 μm (A; all images are the same magnification); 50 μm (B,C); 10 μm (D,E).

keratinocytes exhibit normal motility and ability to form filopodia and lamellipodia as revealed by an in vitro scratch assay.

Accumulation of actin fibers is not observed in epithelial leading edge cells

To test whether FGF10 also regulates actin polymerization in the developing eyelid epithelium, we examined the formation of actin filaments in the eyelid tissues of E15 fetuses. In both wild-type and *Fgf10*$^{+/-}$ fetuses, the eyelid epithelial cells developed prominent F-actin networks as demonstrated by whole-mount phalloidin staining (Fig. 7A,D-F). By contrast, in the homozygous mutant, only a few cells that were mostly confined to a single cell layer at the eyelid tip, formed actin cables (Fig. 7G). Histological sections revealed that F-actin accumulated in the leading edge cells of the wild type (Fig. 7B,C), but not of the mutant (Fig. 7H,I). These results demonstrate that FGF10 regulates actin stress fiber formation in epithelial leading edge cells of the developing eyelid, which is probably associated with epithelial movement and eyelid closure.

Since cell polarization is used to mediate physical fates, as in orientated cell migration (for review, see Macara, 2004), we further examined the polarity of the eyelid epithelial cells in *Fgf10*-null eyelid tips. We performed immunostaining of γ-tubulin to reveal a centrosome: a microtubule-organizing center (MTOC), localized apically in the epithelial cell (Rizzolo and Joshi, 1993). The initial stratification of the single-layer ectoderm during embryonic development gives rise to an outer periderm layer and an inner basal layer. In the wild type, γ-tubulin was localized in the apical side of the epidermal cells in the basal layer (Fig. 7J). It is known that migrating sheets of cells recognize the direction of migration and polarize so that protrusive activity is restricted to the front, and that the MTOC re-orients itself in front of the nucleus to face the direction of migration (Etienne-Manneville and Hall, 2002). Notably, under the experimental conditions employed here, γ-tubulin expression was not observed in the leading edge cells, the periderm cells, but rather in the inner basal layer of the epidermis (Fig. 7J,J′). This finding might be related to the fact that the eyelid epithelial cells lose their typical apicobasal polarity by degrees in migration, as is found in the epithelial-mesenchymal transition, or that the expression was just obscured by unknown factors. Even in the *Fgf10*$^{-/-}$ mutant eyelid, the inner basal layer exhibited γ-tubulin expression apically in the cell (Fig. 7K,K′); however, one row of basal cells appeared wavy, and the number of γ-tubulin-expressing cells seemed to decrease (n=4). Although we found some variability in the expression pattern of γ-tubulin, depending on the developmental stages of eyelid extension and/or the embryos, these results suggest that polarity of the epidermal cells is initially established but later impaired to some extent without FGF10.

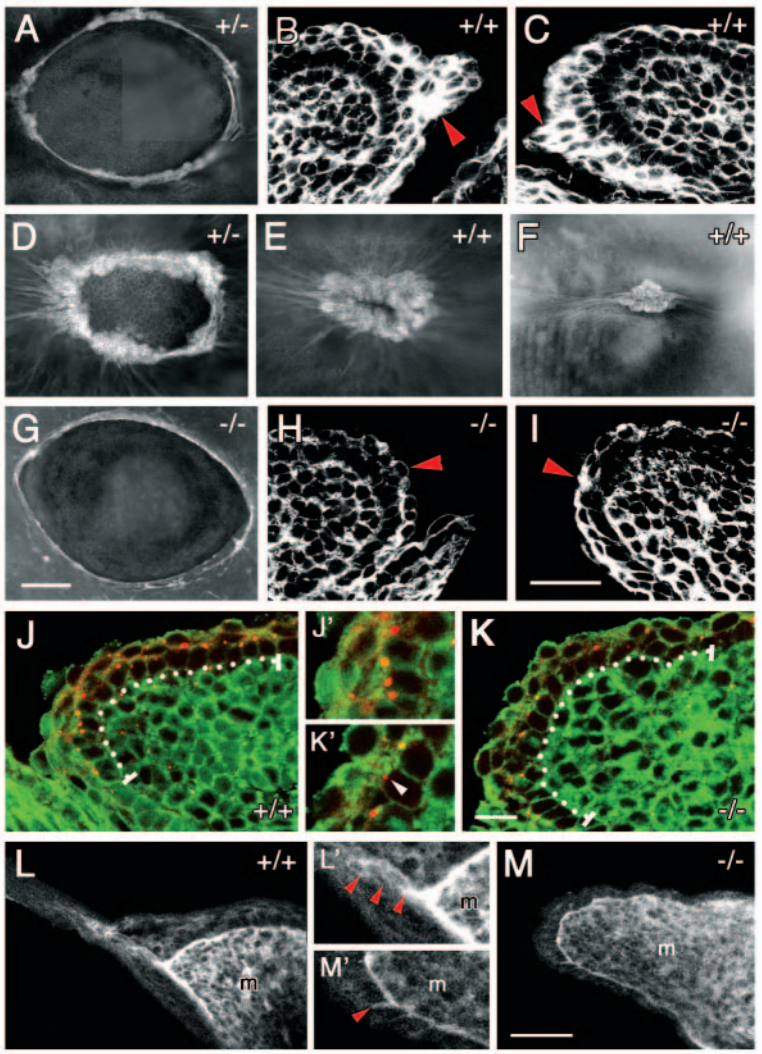

Fig. 7. FGF10 controls actin fiber formation (A-I), cell polarity (J-K) and expression of vimentin (L-M) in the developing eyelid epithelium. Whole-mount (A, D-G) and section (B,C,H,I) staining for F-actin of the eyes from wild-type, *Fgf10*$^{+/-}$ and *Fgf10*$^{-/-}$ fetuses at E15 (A-D,G-M) and E16 (E,F). The upper (B,H) and lower (C,I,J-M) eyelid primordia are shown. (A,D-F) The accumulation of actin fibers at the eyelid leading edge is accelerated, as eyelid closure proceeds. (B,C) Actin fibers are accumulated in the leading edge cells (arrowheads). (G-I) The Rhodamine-phalloidin binding to F-actin is much less on the eyelid margin and in the epithelial leading edge (arrowheads in H and I) of *Fgf10*-null fetuses. (J-K) Immunofluorescence of γ-tubulin. (J,K) The localization of γ-tubulin is indicated by the red, dotted signals. The borders of the cells are shown in green (Bodipy-ceramide). The expression of γ-tubulin in the inner basal layer (along the dotted line; approximately 17 cells were assessed) appears disorganized and reduced in the *Fgf10*$^{-/-}$ eyelid (K). (J′,K′) Higher magnifications of the eyelid tips shown in J and K, respectively. Weak expression of γ-tubulin is detected apically in the mutant epidermal cells (arrowhead in K′). (L,M) Immunofluorescence of vimentin. Note that high levels of vimentin protein are expressed in the eyelid mesenchyme (m). (L) In the wild type, vimentin is also localized in the leading edge epidermal cells. (M) Mutant eyelid epidermal cells express much lower levels of vimentin. (L′,M′) Higher magnifications of the eyelid tip shown in L and M, respectively. The arrowheads indicate the expression of vimentin. All images except A,D-G, which were obtained with a fluorescence stereomicroscope, were captured by laser scanning confocal microscopy. Scale bars: 300 μm (A,D-G); 25 μm (B,C,H,I); 25 μm (J,K); 50 μm (L,M).

Epithelial to mesenchymal transition (EMT) is a crucial morphogenetic process in animal development, in which epithelial cells become motile and mesenchymal in form, losing both their typical apicobasal polarity and their regular arrayed structure. This transition is observed in many developmental processes, such as gastrulation, formation of neural crest cells and fusion process of two primordia such as heart and palate (Savagner, 2001). The development of the eyelid involves temporary fusions of the epithelial layers. To know whether an EMT-like transition might be observed during the eyelid epithelial fusion, we next examined the expression pattern of vimentin in the leading edge migratory eyelid epithelial cells. The intermediate filament protein vimentin is a marker of mesenchymal cells (Savagner, 2001). In agreement, vimentin was expressed by a small population of epithelial cells at the advancing margin of the eyelid, as well as in the eyelid mesenchyme at E15 (Fig. 7L,L′) (n=5). In the mutant eyelid tip, there was positive staining for vimentin, but staining was less extensive than in wild-type embryos at an equivalent stage of migration (Fig. 7M,M′) (n=3). Taken together, these results indicate that the EMT-like transition seems to be involved in temporary eyelid epithelial fusion and is blocked to some extent in eyelid migratory epithelial cells with disrupted FGF10 signaling.

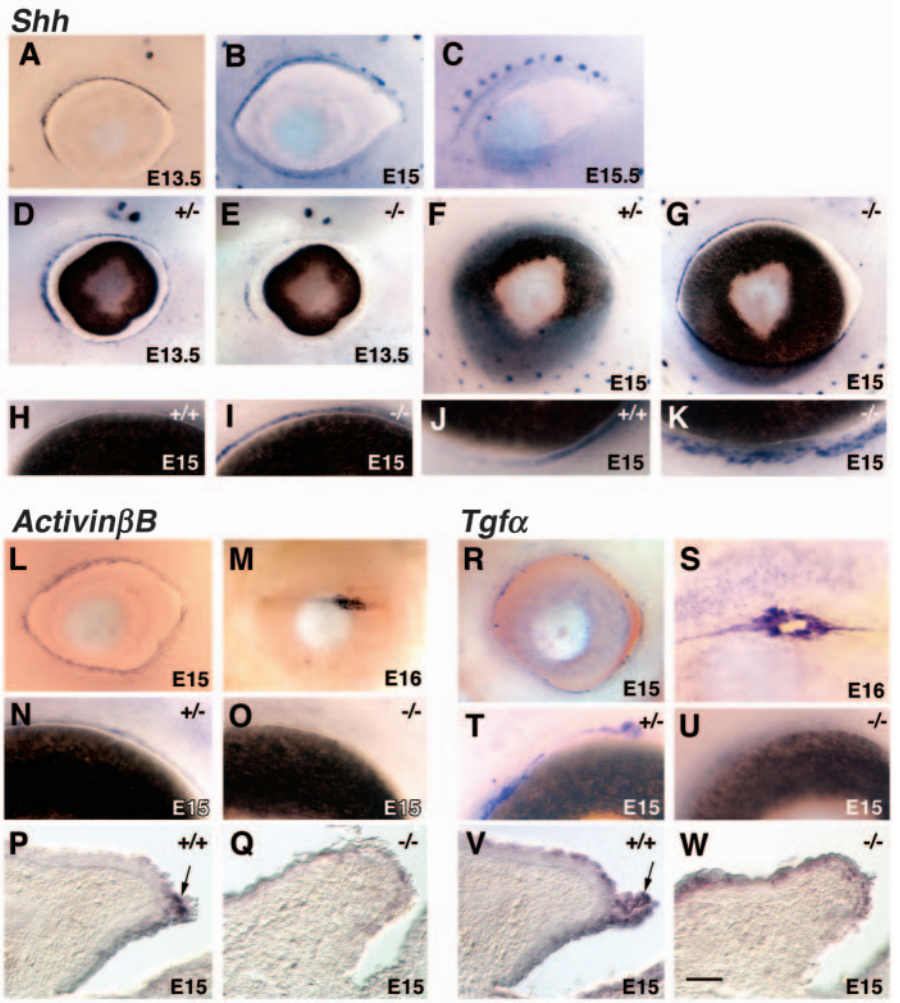

Fig. 8. Expression of *Shh*, activin βB, and *Tgfa* during eyelid closure of normal and *Fgf10*-null mice. To better visualize the normal expression pattern, a mouse strain with no pigment in the eye was used, as shown in A-C,L,M,R,S. Whole-mount in situ hybridization of the eyes (A-O, R-U) and section in situ hybridization of the upper eyelid primordia (P,Q,V,W). Higher magnifications of the upper (H,I,N,O,T,U) and lower (J,K) eyelid margins. In A-O, R-U, the inner canthus is to the right, with the outer canthus to the left. (A-C) *Shh* is expressed along the upper eyelid margin and the temporal canthus at E13.5. By E15, *Shh* expression is also detected along the lower eyelid margin and in the prospective upper eyelash. Shortly after that, *Shh* expression along the eyelid margin becomes down-regulated and restricted to the eyelash anlagen. (D-G) The onset of *Shh* expression along the eyelid margin is delayed in $Fgf10^{-/-}$ mutants. The eyes shown in D,E and F,G were from the same littermates, respectively, and were processed for in situ hybridization simultaneously. In *Fgf10*-null eyelids, *Shh* expression appears down-regulated at E13.5 (E) and up-regulated at E15 (G,I,K), as compared with normal eyelids (D,F,H,J). (L,P) At E15, activin βB is expressed by the leading edge cells (arrow in P) on the eyelid margin, the future periderm cells. (M) By E16, activin βB is expressed by the periderm cells at the fusion line. (N-Q) The expression of activin βB is down-regulated on the *Fgf10*-null eyelid margin, as compared with normal littermates. (R,V) *Tgfa* mRNA is concentrated in the leading edge cells (arrow in V) on the eyelid margin, the future periderm cells. (S) By E16, *Tgfa* is expressed by the periderm cells of the fusing eyelids. (T-W) The expression of *Tgfa* is down-regulated or more diffuse at the *Fgf10*-null eyelid margin, as compared with normal littermates. Scale bars: 50 μm (P,Q,V,W).

The onset of *Shh* expression is delayed in *Fgf10*-null eyelid epithelia

It was reported that *Shh*, *Ptch1* and *Ptch2* are expressed in the developing mouse eyelid at E14.5 (Motoyama et al., 1998). We re-examined the expression of *Shh* in the eyelid epithelium at E13.5 (Fig. 8A), and histological sections verified that *Shh* is expressed by the basal epithelium abutting the dermis as reported previously (Motoyama et al., 1998) (data not shown). Interestingly, more abundant expression of *Shh* was seen on the upper eyelid margin and in the outer canthus region (n=4). By E15.5, expression of *Shh* was found along the eyelid margin and dotted expression was observed on the upper eyelid margin, corresponding to eyelash anlagen (Fig. 8B,C; n=3). *Ptch1* and *Ptch2* were also expressed on the margin of the developing eyelid at E13.5, and more intensely in the upper eyelid and in the outer canthus region (data not shown). By E15.5, *Ptch1* and *Ptch2* were expressed in the putative eyelash primordia (not shown). Thus, the expression patterns of *Fgf10* and *Shh* signaling molecules appears complementary to some extent: *Fgf10* expression is expressed in the mesenchyme and is more intense in the lower eyelid (Fig. 2G), whereas *Shh*, *Ptch1* and *Ptch2* are expressed

in the epithelium (Motoyama et al., 1998), and more intensely in the upper eyelid.

We then examined the expression patterns of *Shh*, *Ptch1* and *Ptch2* in *Fgf10*-null eyelid primordia. As expression of the three genes was similar only *Shh* is shown. At E13.5, expression of *Shh*, *Ptch1* and *Ptch2* was observed on the mutant eyelid margin at a very low level (n=3 for each gene) (Fig. 8E; D, control; data not shown for *Ptch1, Ptch2*). Around E15, however, these genes became expressed along the eyelid margin in the mutant (Fig. 8G; F, control). The expression levels of all three genes appeared to increase on the mutant eyelid margin as compared with the wild type (Fig. 8I; H, control) (n=3). Furthermore, in the wild-type eyelid the *Shh*-expressing cells were kept compact on the lower margin (Fig. 8J), whereas the cells were scattered on the mutant eyelid margin (Fig. 8K). In a later stage at E16.5, however, the expression patterns of *Shh*, *Ptch1* and *Ptch2* were not dotted, as the eyelid remained wide open and eyelash primordia did not develop (not shown). Thus, in the absence of FGF10, the onset of gene expression for *Shh*, *Ptch1* and *Ptch2* is delayed. In addition to impaired growth of the eyelid protrusion, the impaired expression of SHH signaling molecules supports the notion that *Fgf10*-null eyelid primordia have defects by E13.5.

The expression of activin βB and *Tgfa* is not concentrated in the epithelial leading edge cells

Since morphological analysis indicated that the integrity of epithelial leading edge cells of the eyelid primordia was disrupted in the absence of FGF10, we examined the expression of such peridermally expressed genes as activin βB and *Tgfa*. We chose activin βB and *Tgfa* as the mice deficient in these genes exhibit open eyelids at birth (Vassalli et al., 1994; Matzuk et al., 1995; Luetteke et al., 1993; Mann et al., 1993). In normal embryos at around E15, activin βB expression was detected on the eyelid margin (Fig. 8L). Section in situ hybridization indicated that activin βB was expressed in the leading edge of the eyelid epithelium (Fig. 8P). At around E16, the expression of activin βB was observed in the periderm of the fusion line (Fig. 8M). In the *Fgf10*-null eyelid at E15, however, activin βB expression was down-regulated (Fig. 8O; N for comparison). Section in situ hybridization indicated that activin βB was diffusely expressed in the eyelid epithelium at a very low level (Fig. 8Q).

We next examined the expression of *Tgfa* and *Egfr*; mice lacking these genes have no eyelids (Miettinen et al., 1999; Threadgill et al., 1995). *Tgfa* was expressed in the leading edge epithelial cells of normal eyelids (Fig. 8R) and later in the fusion line and the adjacent periderm (Fig. 8S) (Berkowitz et al., 1996). Since *Egfr* was diffusely expressed in the epithelium (data not shown) (Berkowitz et al., 1996), we examined the expression of *Tgfa* as a peridermal marker gene rather than *Egfr*. *Tgfa* expression was down-regulated in the mutant periderm and was not concentrated in the leading edge cells (Fig. 8U,W; T,V, control).

FGF10 protein can up-regulate the expression of activin βB and *Tgfa* in the normal eyelid epithelium and retrieve the eyelid epithelial extension in the *Fgf10*$^{-/-}$ eyelid anlagen

To determine whether the absence of FGF10 protein is directly involved in eyelid defects in *Fgf10*-null mice, we carried out an explant culture of normal eyelid anlagen and implanted an FGF10-soaked bead in the mesenchyme of the lower eyelid. We examined whether activin βB and *Tgfa* were up-regulated or ectopically induced after FGF10-bead application in normal eyelid anlagen. We found that within 12 hours, activin βB (Fig. 9B,C; A,E for comparison) and *Tgfa* (Fig. 9H,I; G,J for comparison) were ectopically induced in the thickened epidermis of the FGF10-bead-implanted eyelid (Fig. 9D; F for comparison). Furthermore, the area showing accumulation of F-actin in the leading edge appeared enlarged after FGF10 application, although no ectopic accumulation was observed near the bead (n=4) (Fig. 9K; L for comparison). By contrast, *Shh* was not ectopically induced by FGF10 protein in the eyelid explants derived from E15 mice (data not shown).

We next assessed whether FGF10 beads could promote epithelial extension in cultured *Fgf10*-null eyelids by applying quantitative morphometry. We measured the area of the eyelid epithelium covering the cornea before and after FGF10-soaked or PBS-soaked bead application, as shown in Fig. 9M. Although FGF10 did not notably promote epithelial extension in the wild-type eyelid anlagen (data not shown), the area of epithelial extension after FGF10 application was considerably wider than that for the PBS-soaked bead on the mutant eyelid anlagen (Fig. 9N). These results indicate that FGF10 can up-regulate the expression of activin βB and *Tgfa* in the normal eyelid epithelium and retrieve the eyelid epithelial extension in the *Fgf10*$^{-/-}$ eyelid anlagen.

Discussion

We have reported the expression pattern of *Fgf10* during embryonic eyelid development and the eyelid defects in *Fgf10*-null mice. *Fgf10* is expressed in the eyelid mesenchyme from the initiation phase of eyelid development. The nascent eyelid epithelia of *Fgf10*-null mice have defects in proliferation and later in the integrity of the eyelid periderm forming on the eyelid margin. *Fgf10*-null keratinocytes exhibit normal motility, and the formation of filopodia and lamellipodia in a scratch assay. Actin fibers, the gene products of activin βB and *Tgfa*, however, are not accumulated or up-regulated in the epithelial leading edge cells of *Fgf10*-deficient eyelids, and the onset of *Shh* expression is delayed in the mutant eyelid epithelium. In an explant culture, the addition of FGF10 protein can up-regulate the expression of activin βB and *Tgfa* in normal eyelid epithelia and retrieve the eyelid epithelial extension, to some extent, in the *Fgf10*$^{-/-}$ eyelid anlagen. These results show that FGF10 has a dual role in embryonic eyelid development, in that it is required for both proliferation (Fig. 10A) and coordinated migration of epithelial leading edge cells (Fig. 10B).

Phenotypic differences in eyelids among *Fgfr2 IgIII*-deleted, *Egfr*-null, *Tgfa*-null and *Fgf10*-null mice

Here, we compare the phenotype of open eyelids at birth found in representative mutants with that of *Fgf10*-null mice. First, the failure of eyelid induction in *Fgfr2 IgIII*-deleted embryos initiates much earlier and more severely than in *Fgf10*$^{-/-}$ mutants; no grooves are formed above or below the eye, indicating that the loss of all FGFs-FGFR2 signaling blocks eyelid formation at its earliest stages (Li et al., 2001). By contrast, in *Fgf10*$^{-/-}$ mutants, shallow but distinct eyelid

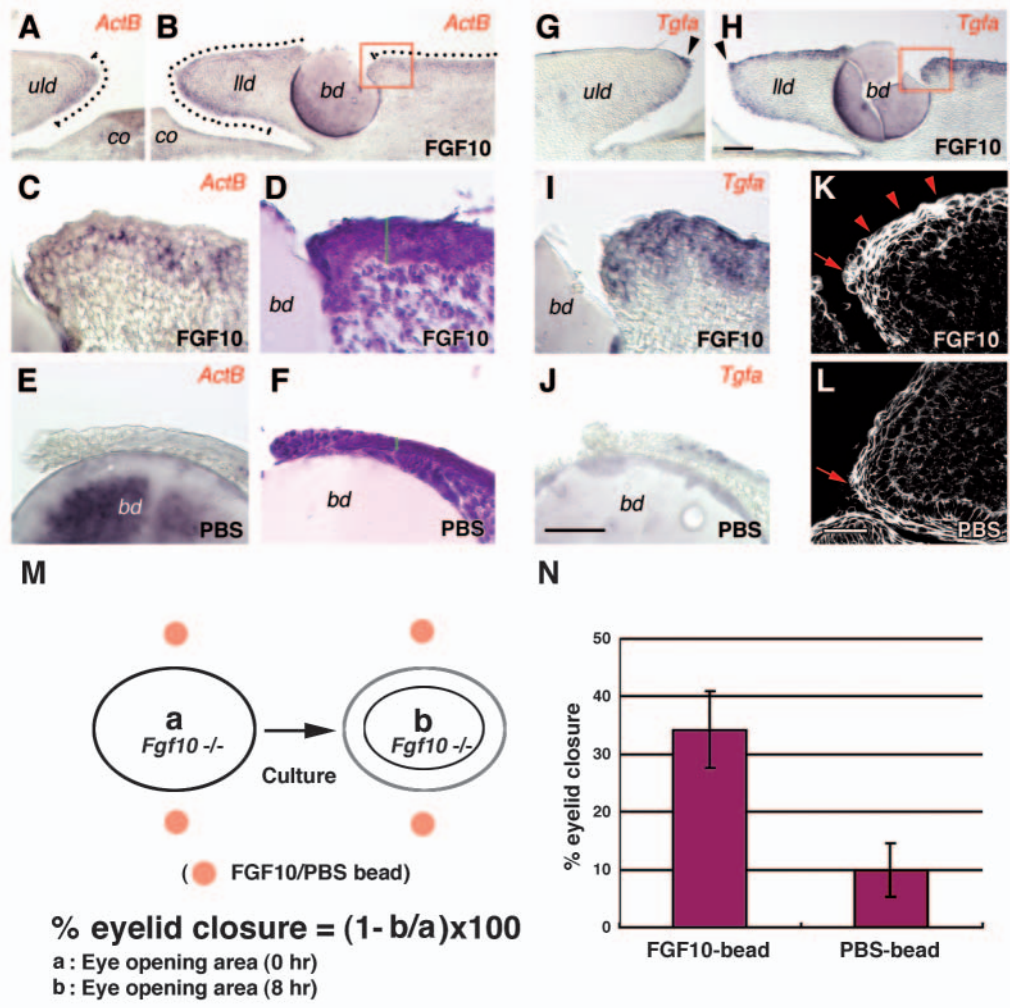

Fig. 9. FGF10 protein induces up-regulation of activin βB and *Tgfa* mRNAs and promotes eyelid closure in an explant culture. An FGF10- or PBS-soaked bead was implanted in the eyelid mesenchyme. The expression patterns of activin βB, *Tgfa* and F-actin were examined 12 hours after the culture of E15 normal eyelid anlagen. (A-D) The expression domain of activin βB (indicated by the dotted lines in A and B) was enlarged after FGF10 bead implantation (B). (C) Higher magnification of the area boxed in B. Activin βB is expressed by subsets of cells in the thickened epidermis after FGF10 application. (D) Histology of a serial section of the explant shown in C and I. The epidermis (shown by the green line) in the vicinity of an FGF10 bead was thickened, as compared with that in F. (E) Activin βB is not expressed in the normal epidermis abutting a PBS bead. (F) Histology of a serial section of the explant shown in E and J. Normal thickness of the epidermis is indicated by the green line. (G-J) The expression domain of *Tgfa* is enlarged after FGF10-bead implantation (H). The arrowhead in G and H indicates the leading edge of the eyelid. (I) *Tgfa* is distinctly expressed in the thickened epithelium abutting the FGF10-bead. (K,L) Phalloidin staining of the eyelid tips after FGF10-bead (K) or PBS-bead (L) implantation. The area showing accumulation of F-actin is enlarged after FGF10 application (arrowheads in K). The arrows in K and L indicate the epithelial leading edge. (M) Schematic representation of an explant culture of *Fgf10*-null eyelid anlagen and calculation of the percentage of eyelid closure after FGF10 application. The area of the eyelid opening was measured before and after the culture. Two beads were implanted in the eyelid mesenchyme. (N) FGF10 protein can promote eyelid closure in the *Fgf10*-null eyelid anlagen. ActB, activin βB; bd, bead; co, cornea; lld, lower eyelid; uld, upper eyelid. Scale bars: 100 μm (A,B,G,H); 50 μm (C-F,I,J); 50 μm (K,L).

grooves are formed and epithelial ridge formation is initially observed, although the eyelid protrusion is smaller and the integrity of peridermal clumps is disrupted. Thus, it is conceivable that multiple ligands of FGFR2 must be involved in eyelid development, among which FGF10 is critical for proliferation and maintenance of peridermal clumps at the leading edge of the developing eyelid margin. The residual signaling by FGFR2 *via* FGF10-related molecules such as FGF7 is likely to function in the absence of FGF10 and thus the phenotype of *Fgf10*-null eyelids must be milder than that in FGFR2b-null eyelids.

The EGF receptor (EGFR) is activated upon binding of a family of polypeptides that includes EGF, TGFα, amphiregulin, heparin-binding EGF, betacellulin and epiregulin. *Egfr*-null mice have open eyelids at birth (Miettinen et al., 1995), whereas *Tgfa* null mice display a failure or a delay in prenatal eyelid growth and fusion (Berkowitz et al., 1996). This indicates the importance of TGFα-EGFR signaling in prenatal eyelid development and that other ligands of EGFR could also elaborate eyelid development. The eyelids of *Tgfa* null embryos exhibit variable extension across the cornea but no contact with the opposing epithelia (Berkowitz et al., 1996). This phenotype appears milder than that found in *Fgf10*-null mice, as *Fgf10*-null mice have open eyelids in which epithelial extension is not observed. Taken together with the down-regulation of *Tgfa* gene expression in the absence of FGF10, the *Tgfa* gene may be a target of the FGF10 signaling during early eyelid development.

The expression analysis of *Tgfa* and *Egfr* revealed that both genes are expressed in the developing eyelid epithelium: *Tgfa* mRNA is concentrated in the distal tips of the eyelids, whereas *Egfr* mRNA is prevalent throughout the epithelia on the eyelids and the cornea (Berkowitz et al., 1996). This implies that the TGFα-EGFR signaling may be involved in eyelid development in an autocrine or juxtacrine mode. By contrast, *Fgf10* is expressed in the eyelid mesenchyme, while its receptor gene

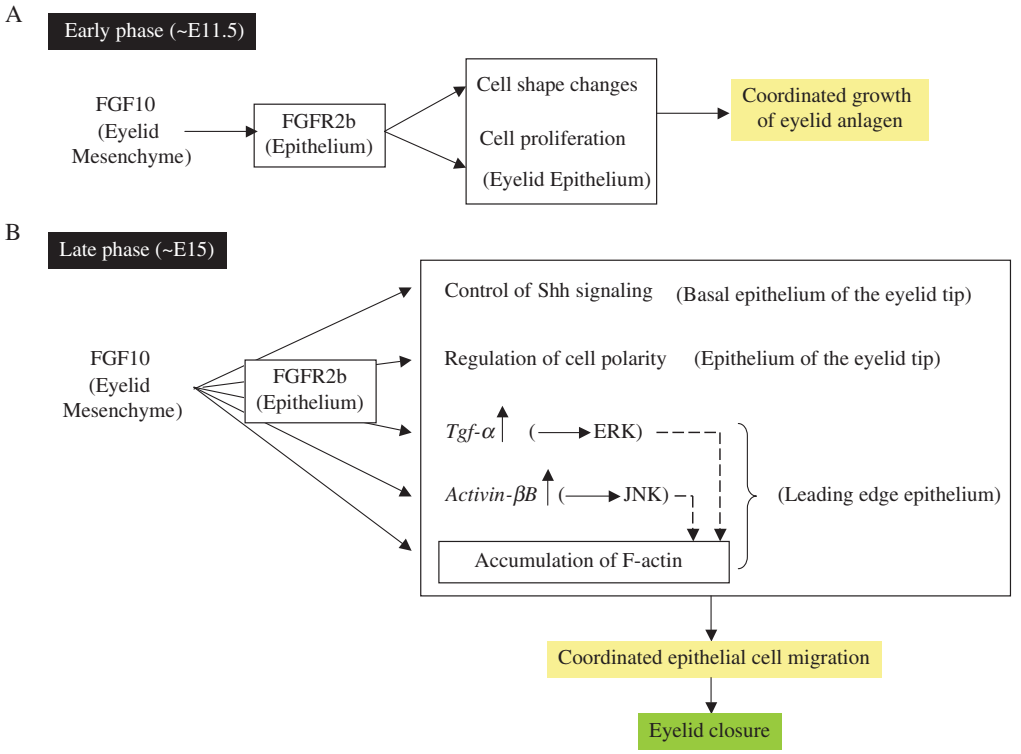

Fig. 10. A dual role for FGF10 in controlling mouse eyelid development. (A) In the early phase of eyelid development, FGF10-FGFR2b signaling is required for cell shape changes and proliferation of the prospective eyelid epithelium, leading to coordinated growth of the eyelid anlagen. (B) In the late phase, FGF10-FGFR2b signaling is involved in up-regulation of *Tgfa* and activin βB, and accumulation of F-actin in the epithelial leading edge cells, thus directing epithelial cell migration, epithelial sheet movement, and eyelid closure. The pathways indicated by the broken lines are suggested by other studies (for review, see Xia and Kao, 2004). It is not known whether FGF10 could directly regulate the accumulation of F-actin or indirectly through TGF-α and/or activin pathways. This study has shown that FGF10 is necessary for proper expression of *Shh* in the basal layer of the eyelid tip epidermis (Motoyama et al., 1998), and for the integrity of the cell polarity of the eyelid basal epidermis. FGF10-FGFR2b signaling orchestrates these genetic and cellular activities during mouse eyelid fusion processes. These molecular interplays indeed result from combinatorial regulation of FGF10 and other extrinsic and intrinsic factors, which define the developmental context of developing eyelids. Other ligands of FGFR2b must be required for growth of the eyelid anlagen, as well.

Fgfr2b is expressed in the epithelium (Li et al., 2001) (Fig. 2J-M), indicating that FGF10-FGFR2b acts in a paracrine manner between the epithelium and the mesenchyme. This suggests that there are two important tissue interactions during eyelid formation: intra-epithelial and epithelial-mesenchymal, mediated by TGFα-EGFR and FGF10-FGFR2b signaling, respectively. Since it has been shown that TGFα stimulates keratinocyte proliferation and migration (Barrandon and Green, 1987), it is possible that some functions of FGF10 in eyelid formation, such as eyelid epithelial proliferation and migration could be mediated by TGFα signaling.

FGF10 is likely to oppose SHH signaling in eyelid epithelial migration

SHH is a counterpart of *Drosophila* Hedgehog (Hh), a secreted molecule implicated in the formation of embryonic structures and in tumorigenesis. The Patched (PTCH1) protein, constituting a receptor complex for Hh molecules is thought to oppose Hh signals by repressing the transcription of genes that can be activated by Hh. In vertebrates, two types of PTCH molecules, PTCH1 and PTCH2, have been identified and transcriptional regulation between SHH and PTCH has been reported (Marigo and Tabin, 1996; Goodrich et al., 1996). This study has demonstrated, in the absence of FGF10 signaling, that there is a delay in its interpretation for induction of *Shh* expression. Distinct *Shh* expression in the mutant eyelid at E15 is reminiscent of its capability to restrict adhesion and migration, as reported for neural crest cells (Testaz et al., 2001). Since conventional *Shh* or *Ptch1* knockout mice were shown to suffer from severe developmental defects, the precise role of SHH signaling in eyelid development is still unclear. However, Motoyama et al. (Motoyama et al., 1998) showed that *Shh*, *Ptch1* and *Ptch2* are expressed in the basal epithelium of developing eyelids, but not in the mobile periderm. Taken together, it is conceivable that activation of SHH signaling might antagonize cell migration, and that it should be down-regulated when the primitive periderm cells start to stream onto the ocular surface under the control of FGF10 signaling.

FGF10 signaling links to activin and TGFα signaling

The activin βB gene encodes the activin/inhibin βB subunit, constituting the dimeric growth factors of activin B, activin AB and inhibin B, which belong to the TGFβ family. Mice deficient in activin βB are viable but have defective eyelid development (Vassalli et al., 1994; Matzuk et al., 1995). This study showed peridermal expression of activin βB and *Tgfa*,

their down-regulation in *Fgf10*-null eyelid primordia and up-regulation of expression by the FGF10 protein. Thus, it is likely that activin βB is a downstream component of FGF10 signaling during embryonic eyelid development. Given that activin and basic FGF have been shown to control cell migration in the *Xenopus* gastrula (Wacker et al., 1998), FGF10 might be involved in cell migration by interacting with activin signaling during mouse eyelid development.

Studies of mice with open eyelids at birth have shown that embryonic eyelid closure requires at least two signaling pathways, involving activin-MEKK1-JNK/p38 and TGFα/EGFR-ERK (Zhang et al., 2003; Xia and Kao, 2004). The known end point of the former pathway is actin stress fiber formation and phosphorylation of the nuclear factor Jun, the expression or activity of which might be of importance for the induction of EGFR and the activation of the second pathway. Although expression of activin βB and *Tgfa* is found in *Fgf10*-null eyelid epithelia at a low level, their mRNAs are not accumulated in leading edge cells without FGF10. Thus, this study further supports the notion that FGF10 positively regulates these signaling pathways during mouse eyelid closure. It is not known whether the control of mRNA distribution of activin βB and Tgfa and the accumulation of F-actin through FGF10 signaling are correlated or parallel pathways.

Cellular events mediated by FGF10 during eyelid closure

Recently, it has been thought that mammalian eyelid fusion is one of the developmental models for epidermal hole/wound closure, re-epithelialization and even wound healing to some extent, as is the case for dorsal closure in *Drosophila* embryos. There are two modes of epidermal hole/wound closure: actin purse-string mode and lamellipodial crawling mode (Martin and Parkhurst, 2004). In the actin purse-string mode, during the phase of epithelial sweeping, the leading edge cells accumulate actin and myosin just beneath the cell membrane at their apical edge. This F-actin accumulation forms a contractile cable, which pulls the leading edges (LEs) of the epithelial sheets taut (Jacinto et al., 2002) and drives LE cell apical constriction before further elongation and migration of the LE cells (Martin and Parkhurst, 2004). Since accumulation of actin fibers in LE cells was not observed in *Fgf10*-null eyelids, while the scratch assay of cultured mutant keratinocytes showed the formation of lamellipodia, FGF10 may be required for a kind of wound-healing process by the actin purse-string mode rather than by the lamellipodial crawling mode. Furthermore, FGF10 signaling appears to have a role in maturation of filopodia in migrating eyelid epithelial cells.

The epithelial cells of $Fgf10^{-/-}$ mutant eyelids exhibit a polarity (shown by γ-tubulin expression) and form prospective periderm cells, suggesting that even in the absence of FGF10 signaling the polarization signal is received by the eyelid LE cells, but that there is a collapse in its integrity without FGF10. This suggests that FGF10 makes the eyelid LE cells competent to maintain a pre-existing polarization signal.

Concluding remarks

The permissive function of FGF10 signaling translates into the correct coordination of different events in eyelid development, i.e. cell shape changes and proliferation in the early phase (Fig. 10A), and cell migration and polarity in the late phase, by regulating the activity of cytoskeleton and gene transcription (Fig. 10B). In the absence of FGF10, the leading edge cells cannot elongate centripetally, and these defects may well be responsible for the failure of $Fgf10^{-/-}$ eyelid epidermis to spread over the developing cornea. This study also suggests mouse eyelid epithelial fusion as a new paradigm to elucidate the mechanisms of EMT. It has been reported that several members of the Wnt family are expressed in the developing eyelid primordia of the mouse (Liu et al., 2003). Although the phenotype of open eyelids at birth has not so far been reported for any Wnt mutants, a Wnt pathway was shown to be involved in *Drosophila* dorsal closure (Morel and Arias, 2004). It is therefore tempting to speculate that a Wnt pathway might be related to FGF10 signaling in mouse eyelid development.

Embryonic wound healing is a rapid process (taking place within 1 day in the case of eyelid closure) involving actin cable formation but no apparent hemostatic or inflammatory response (Martin and Lewis, 1992). Therefore, further elucidation of the mechanisms of eyelid closure will be useful in guiding us to better control the cell behaviors of repair in a clinical scenario.

We are grateful to G. Li and R. S. Johnson for information on the mouse keratinocyte culture. We also thank K. Tsuchida and J. Motoyama for providing reagents, and T. Adachi and K. Ohata for technical assistance. The monoclonal antibody used in this study was obtained from the Developmental Studies Hybridoma Bank developed under the auspices of the NICHD and maintained by the University of Iowa, Department of Biological Sciences, Iowa City, IA 52242, USA. This study was partly supported by Grants in Aid for Scientific Research from the Ministry of Education, Culture, Sports, Science and Technology of Japan, and by the Tanabe Medical Frontier Conference (TMFC).

References

Barrandon, Y. and Green, H. (1987). Cell migration is essential for sustained growth of keratinocyte colonies: the roles of transforming growth factor-alpha and epidermal growth factor. *Cell* **50**, 1131-1137.

Berkowitz, E. A., Seroogy, K. B., Schroeder, J. A., Russell, W. E., Evans, E. P., Riedel, R. F., Phillips, H. K., Harrison, C. A., Lee, D. C. and Luetteke, N. C. (1996). Characterization of the mouse transforming growth factor alpha gene: its expression during eyelid development and in waved 1 tissues. *Cell Growth Differ.* **7**, 1271-1282.

Celli, G., LaRochelle, W. J., Mackem, S., Sharp, R. and Merlino, G. (1998). Soluble dominant-negative receptor uncovers essential roles for fibroblast growth factors in multi-organ induction and patterning. *EMBO J.* **17**, 1642-1655.

De Moerlooze, L., Spencer-Dene, B., Revest, J., Hajihosseini, M., Rosewell, I. and Dickson, C. (2000). An important role for the IIIb isoform of fibroblast growth factor receptor 2 (FGFR2) in mesenchymal-epithelial signalling during mouse organogenesis. *Development* **127**, 483-492.

Etienne-Manneville, S. and Hall, A. (2002). Rho GTPases in cell biology. *Nature* **420**, 629-635.

Findlater, G. S., McDougall, R. D. and Kaufman, M. H. (1993). Eyelid development, fusion and subsequent reopening in the mouse. *J. Anat.* **183**, 121-129.

Goodrich, L. V., Johnson, R. L., Milenkovic, L., McMahon, J. A. and Scott, M. P. (1996). Conservation of the hedgehog/patched signaling pathway from flies to mice: induction of a mouse patched gene by Hedgehog. *Genes Dev.* **10**, 301-312.

Harris, M. J. and McLeod, M. J. (1982). Eyelid growth and fusion in fetal mice. A scanning electron microscope study. *Anat. Embryol. (Berl)* **164**, 207-220.

Harris, M. J. and Juriloff, D. M. (1986). Eyelid development and fusion

induced by cortisone treatment in mutant, lidgap-Miller, foetal mice. A scanning electron microscope study. *J. Embryol. Exp. Morphol.* **91**, 1-18.

Jacinto, A., Wood, W., Woolner, S., Hiley, C., Turner, L., Wilson, C., Martinez-Arias, A. and Martin, P. (2002). Dynamic analysis of actin cable function during *Drosophila* dorsal closure. *Curr. Biol.* **12**, 1245-1250.

Juriloff, D. M. and Harris, M. J. (1989). A scanning electron microscope study of fetal eyelid closure accelerated by cortisone in SWV/Bc mice. *Teratology* **40**, 59-66.

Kume, T., Deng, K. Y., Winfrey, V., Gould, D. B., Walter, M. A. and Hogan, B. L. (1998). The forkhead/winged helix gene Mf1 is disrupted in the pleiotropic mouse mutation congenital hydrocephalus. *Cell* **93**, 985-996.

Lele, Z., Folchert, A., Concha, M., Rauch, G. J., Geisler, R., Rosa, F., Wilson, S. W., Hammerschmidt, M. and Bally-Cuif, L. (2002). parachute/n-cadherin is required for morphogenesis and maintained integrity of the zebrafish neural tube. *Development* **129**, 3281-3294.

Li, C., Guo, H., Xu, X., Weinberg, W. and Deng, C. X. (2001). Fibroblast growth factor receptor 2 (Fgfr2) plays an important role in eyelid and skin formation and patterning. *Dev. Dyn.* **222**, 471-483.

Li, G, Gustafson-Brown, C., Hanks, S. K., Nason, K., Arbeit, J. M., Pogliano, K., Wisdom, R. M. and Johnson, R. S. (2003). c-Jun is essential for organization of the epidermal leading edge. *Dev. Cell* **4**, 865-877.

Libusova, L., Sulimenko, T., Sulimenko, V., Hozak, P. and Draber, P. (2004). gamma-Tubulin in Leishmania: cell cycle-dependent changes in subcellular localization and heterogeneity of its isoforms. *Exp. Cell Res.* **295**, 375-386.

Liu, H., Mohamed, O., Dufort, D. and Wallace, V. A. (2003). Characterization of Wnt signaling components and activation of the Wnt canonical pathway in the murine retina. *Dev. Dyn.* **227**, 323-334.

Luetteke, N. C., Qiu, T. H., Peiffer, R. L., Oliver, P., Smithies, O. and Lee, D. C. (1993). TGF alpha deficiency results in hair follicle and eye abnormalities in targeted and waved-1 mice. *Cell* **73**, 263-278.

Macara, I. G. (2004). Parsing the polarity code. *Nat. Rev. Mol. Cell. Biol.* **5**, 220-231.

Mann, G. B., Fowler, K. J., Gabriel, A., Nice, E. C., Williams, R. L. and Dunn, A. R. (1993). Mice with a null mutation of the TGF alpha gene have abnormal skin architecture, wavy hair, and curly whiskers and often develop corneal inflammation. *Cell* **73**, 249-261.

Marigo, V. and Tabin, C. J. (1996). Regulation of patched by sonic hedgehog in the developing neural tube. *Proc. Natl. Acad. Sci. USA* **93**, 9346-9351.

Martin, P. and Lewis, J. (1992). Actin cables and epidermal movement in embryonic wound healing. *Nature* **360**, 179-183.

Martin, P. and Parkhurst, S. M. (2004). Parallels between tissue repair and embryo morphogenesis. *Development* **131**, 3021-3034.

Matzuk, M. M., Kumar, T. R., Vassalli, A., Bickenbach, J. R., Roop, D. R., Jaenisch, R. and Bradley, A. (1995). Functional analysis of activins during mammalian development. *Nature* **374**, 354-356.

Miettinen, P. J., Berger, J. E., Meneses, J., Phung, Y., Pedersen, R. A., Werb, Z. and Derynck, R. (1995). Epithelial immaturity and multiorgan failure in mice lacking epidermal growth factor receptor. *Nature* **376**, 337-341.

Motoyama, J., Heng, H., Crackower, M. A., Takabatake, T., Takeshima, K., Tsui, L. C. and Hui, C. (1998). Overlapping and non-overlapping Ptch2 expression with Shh during mouse embryogenesis. *Mech. Dev.* **78**, 81-84.

Morel, V. and Arias, A. M. (2004). Armadillo/beta-catenin-dependent Wnt signalling is required for the polarisation of epidermal cells during dorsal closure in *Drosophila*. *Development* **131**, 3273-3283.

Ohuchi, H., Hori, Y., Yamasaki, M., Harada, H., Sekine, K., Kato, S. and Itoh, N. (2000). FGF10 acts as a major ligand for FGF receptor 2 IIIb in mouse multi-organ development. *Biochem. Biophys. Res. Commun.* **277**, 643-649.

Pei, Y. F. and Rhodin, J. A. (1970). The prenatal development of the mouse eye. *Anat. Rec.* **168**, 105-125.

Rizzolo, L. J. and Joshi, H. C. (1993). Apical orientation of the microtubule organizing center and associated gamma-tubulin during the polarization of the retinal pigment epithelium in vivo. *Dev. Biol.* **157**, 147-156.

Savagner, P. (2001). Leaving the neighborhood: molecular mechanisms involved during epithelial-mesenchymal transition. *BioEssays* **23**, 912-923.

Sekine, K., Ohuchi, H., Fujiwara, M., Yamasaki, M., Yoshizawa, T., Sato, T., Yagishita, N., Matsui, D., Koga, Y., Itoh, N. and Kato, S. (1999). Fgf10 is essential for limb and lung formation. *Nat. Genet.* **21**, 138-141.

Stepp, M. A. (1999). Alpha9 and beta8 integrin expression correlates with the merger of the developing mouse eyelids. *Dev. Dyn.* **214**, 216-228.

Tao, H., Yoshimoto, Y., Yoshioka, H., Nohno, T., Noji, S. and Ohuchi, H. (2002). FGF10 is a mesenchymally derived stimulator for epidermal development in the chick embryonic skin. *Mech. Dev.* **116**, 39-49.

Testaz, S., Jarov, A., Williams, K. P., Ling, L. E., Koteliansky, V. E., Fournier-Thibault, C. and Duband, J. L. (2001). Sonic hedgehog restricts adhesion and migration of neural crest cells independently of the Patched-Smoothened-Gli signaling pathway. *Proc. Natl. Acad. Sci. USA* **98**, 12521-12526.

Thompson, H. M., Cao, H., Chen, J., Euteneuer, U. and McNiven, M. A. (2004). Dynamin 2 binds gamma-tubulin and participates in centrosome cohesion. *Nat. Cell Biol.* **6**, 335-342.

Threadgill, D. W., Dlugosz, A. A., Hansen, L. A., Tennenbaum, T., Lichti, U., Yee, D., LaMantia, C., Mourton, T., Herrup, K., Harris, R. C. et al. (1995). Targeted disruption of mouse EGF receptor: effect of genetic background on mutant phenotype. *Science* **269**, 230-234.

Uda, M., Ottolenghi, C., Crisponi, L., Garcia, J. E., Deiana, M., Kimber, W., Forabosco, A., Cao, A., Schlessinger, D. and Pilia, G. (2004). Foxl2 disruption causes mouse ovarian failure by pervasive blockage of follicle development. *Hum. Mol. Genet.* **13**, 1171-1181.

Vassalli, A., Matzuk, M. M., Gardner, H. A., Lee, K. F. and Jaenisch, R. (1994). Activin/inhibin beta B subunit gene disruption leads to defects in eyelid development and female reproduction. *Genes Dev.* **8**, 414-427.

Wacker, S., Brodbeck, A., Lemaire, P., Niehrs, C. and Winklbauer, R. (1998). Patterns and control of cell motility in the *Xenopus* gastrula. *Development* **125**, 1931-1942.

Weiss, L. W. and Zelickson, A. S. (1975). Embryology of the epidermis: ultrastructural aspects. II. Period of differentiation in the mouse with mammalian comparisons. *Acta. Derm. Venereol.* **55**, 321-329.

Xia, Y. and Kao, W. W. (2004). The signaling pathways in tissue morphogenesis: a lesson from mice with eye-open at birth phenotype. *Biochem. Pharmacol.* **68**, 997-1001.

Yang, H., Wanner, I. B., Roper, S. D. and Chaudhari, N. (1999). An optimized method for in situ hybridization with signal amplification that allows the detection of rare mRNAs. *J. Histochem. Cytochem.* **47**, 431-446.

Zenz, R., Scheuch, H., Martin, P., Frank, C., Eferl, R., Kenner, L., Sibilia, M. and Wagner, E. F. (2003). c-Jun regulates eyelid closure and skin tumor development through EGFR signaling. *Dev. Cell* **4**, 879-889.

Zhang, L., Wang, W., Hayashi, Y., Jester, J. V., Birk, D. E., Gao, M., Liu, C. Y., Kao, W. W., Karin, M. and Xia, Y. (2003). A role for MEK kinase 1 in TGF-beta/activin-induced epithelium movement and embryonic eyelid closure. *EMBO J.* **22**, 4443-4454.